PERGAMON

International Journal of Heat and Mass Transfer 45 (2002) 67–74

International Journal of HEAT and MASS TRANSFER

www.elsevier.com/locate/ijhmt

Solution to inverse heat conduction problems employing singular value decomposition and model-reduction

J.R. Shenefelt *, R. Luck, R.P. Taylor, J.T. Berry

Department of Mechanical Engineering, Mississippi State University, P.O. Drawer ME, 210 Carpenter Engineering Building, Mississippi State, MS 39762, USA

Received 5 May 2000; received in revised form 2 April 2001

Abstract

A new and simple method for solving linear, inverse heat conduction problems using temperature data containing significant noise is presented in this paper. The method consists in a straightforward application of singular-value decomposition to the matrix form of Duhamel's principle. A physical interpretation of the method is given by discussing the frequency-domain interpretation of the decomposition. Basically, rows and columns are removed from the decomposed matrices that are associated with small singular values that are shown to be associated with frequencies where the signal-to-noise ratio is small. The technique is demonstrated by considering a standard one-dimensional example. Advantages of the new method are reduction in matrix size, robust treatment of noisy temperature data, optimal in the least-squares sense, and lack of ad hoc parameters. © 2001 Published by Elsevier Science Ltd.

1. Introduction

In many situations it is difficult to analytically determine the heat transfer that enters or leaves a heat conducting material. Thermocouples and similar devices, however, allow accurate temperature measurements to be taken in most situations. Such temperature measurements provide the data necessary to determine the surface heat transfer by employing an inverse technique.

Inverse heat conduction problems often are ill-posed problems since small errors in temperature measurements can cause large errors in calculated heat transfer [2]. This problem results from the thermal-damping nature of the heat-conducting material. When a step change in the interfacial heat flux is applied to a heat-conducting material, the temperature response within the material is smooth because of thermal damping. Low-level, broadband noise corrupting the temperature data can result in an unreasonable solution for calculated heat flux.

One of the earliest inverse methods was proposed by Stolz [1] to solve a quenching problem involving a spherical geometry. The method proposed by Stolz used a single future- temperature measurement from a single-temperature sensor to determine the previous heat flux in a time-sequential manner. This process is conducted analytically resulting in a pulse-sensitivity coefficient matrix for heat flux. Since the exact method employs a single future-temperature during each time-step, the method becomes unstable if the time-steps are not sufficiently large. To overcome the possible instability, Beck [2] introduced methods incorporating multiple future temperature measurements. By incorporating data from multiple future time-steps the gain coefficient may vary reducing possible instabilities. More recently Beck [3] has compared the future time-step approach with other inverse methods. Other authors have used methods based on future time-step and parameter-estimation methods proposed by Beck to solve a wide variety of inverse problems [4–7]. Frankel and Keyhani [8] present a global time solution employing a weighted-residual methodology which is proposed that solves the inverse

* Corresponding author. Tel.: +1-662-325-9230; fax: +1-662-325-7223.

E-mail address: shenefelt@me.msstate.edu (J.R. Shenefelt).

0017-9310/02/$ - see front matter © 2001 Published by Elsevier Science Ltd.
PII: S0017-9310(01)00129-6

Nomenclature

c_p	specific heat (J/kg °C)
h	time-step (s)
k	thermal conductivity (W/m °C)
K	matrix of spatial derivatives
m	heat flux pulse magnitude (W/m^2)
M	exponential matrix $= e^{Kh}$
n	number of nodes
N	number of time-steps
R	vector locating heat flux
P	discrete series matrix
q	heat flux vector in time (W/m^2)
S	matrix containing singular values
t	time (s)
T	node temperature (°C)
T	temperature vector (°C)
$\dot{\mathbf{T}}$	time rate of change in temperature vector (°C/s)
U	matrix containing orthonormal columns
V	matrix containing orthonormal columns
x	position (m)

Subscripts

i	node location
new	reduced-order matrices

Superscript

j	time indicator

Greek symbols

α	thermal diffusivity (m^2/s)
Φ	temperature pulse response matrix
ρ	density (kg/m^3)
θ	temperature vector for all time at a given location (°C)

problem over the entire time domain. Recently a number of authors have proposed methods for solving the inverse problem based on dynamic programming and control theory.

Blum [9] converts the heat transfer problem into a dynamic system with an observer and uses the system's frequency response to determine an optimal solution to the inverse problem. The work proposed by Blum shares much similarity to observer modeling done earlier by Marquardt [10]. Bayo uses a finite-element approach incorporating data from the frequency domain using discrete Fourier transforms to obtain the inverse solution [11]. The model is extended to the time domain through the use of a two-sided convolution integral. The method has the advantage of being computationally efficient and does not require a stabilization procedure to be defined. The method does require a digital-filtering technique to be employed to arrive at the inverse-problem solution. Moulin [12] extended the work presented by Bayo to solve nonlinear inverse problems by modifying the model.

Trujillo and Busby [13] use a dynamic-programming approach incorporating a smoothing parameter and least squares to obtain solutions for inverse heat conduction problems. The method proposed by Trujillo and Busby is based on work previously done by Tikhonov and is recognized as Tikhonov's method [14]. Since the observer, smoothing-parameter or digital- filtering technique is often difficult to determine, additional authors have used Kalman filtering approaches to solve the inverse problem.

The Kalman filter is a filtering technique very widely used to solve inverse heat conduction problems [15]. Tuan uses the Kalman filter and a real-time least-squares algorithm to solve a two-dimensional inverse heat conduction problem [16]. Ji successfully demonstrated the Kalman filter on a one-dimensional problem with errors in the measured temperatures by comparing the calculated heat transfer with heat transfer measurements taken experimentally [17].

Ozisik and Orlande [18] report several additional methods that can be employed to solve inverse heat conduction problems. One of the methods reported on is the conjugate gradient method. This method has the advantage of being able to solve both linear and nonlinear problems in a relatively short time period. Colaco and Orlande [19] have compared several different conjugate gradient method approaches when applied to inverse heat conduction problems. Huang and Wang use a conjugate gradient approach to solve a three-dimensional problem [20]. However, the algorithm is computationally intensive, may require large amounts of memory and is unnecessarily complex for the linear case. The methods derived to date either require much iteration and/or memory, the use of ad hoc parameters, or are based on unnecessarily complex explanations of a rather straightforward linear analysis problem. A new, straightforward, simple and effective method is proposed below.

In this paper, the one-dimensional, linear inverse heat conduction problem is solved using the matrix form of Duhamel's principle. A unit heat flux pulse is applied to a linear conduction model and the temperature response is determined. The system response to the unit heat pulse is recorded and employed to investigate the physical problem. A Toeplitz matrix (constant along the diagonals) is assembled using the unit heat pulse response as the first column. Singular-value decomposition is performed on the matrix. Then, the singular values are compared and the matrix is reduced until properly

conditioned. The primary result of the matrix reduction is shown to be filtering of high-frequency fluctuations in the calculated heat flux data. An important characteristic of this method is a pulse response that can be obtained from any acceptable linear conduction model. Thus, the proposed method only requires unit pulse temperature response data that can be easily obtained from accepted software packages. The latter statement becomes increasingly important when extending the results of this work to two- or three-dimensional domains.

The new method allows three advantages when solving linear inverse heat conduction problems. First, the method is able to recover heat flux profiles from temperature data containing a significant amount of noise. Second, the method is based on a unit pulse-temperature response that is defined by the physical problem. Therefore, the solution is only determined by the physical problem and the signal-to-noise ratio. Third, the method provides a solution that is optimal in the least-squares sense [22].

2. Development of the matrix-transform technique

A one-dimensional heat conduction problem, Fig. 1, is used to demonstrate the matrix-transform method. Initially the homogeneous material is at a uniform initial temperature, T_0 ($T_0 = 0$). A transient heat flux is applied at the left boundary ($x = 0$). The right boundary ($x = L$) is insulated, so no energy is lost. This is expressed mathematically

$$\frac{\partial^2 T}{\partial x^2} = \frac{1}{\alpha}\left(\frac{\partial T}{\partial t}\right), \qquad 0 < x < L, \quad t > 0, \tag{1}$$

$$-k\left(\frac{\partial T}{\partial x}\right) = q(t), \qquad x = 0, \quad t > 0, \tag{2}$$

$$\frac{\partial T}{\partial x} = 0, \qquad x = L, \quad t > 0, \tag{3}$$

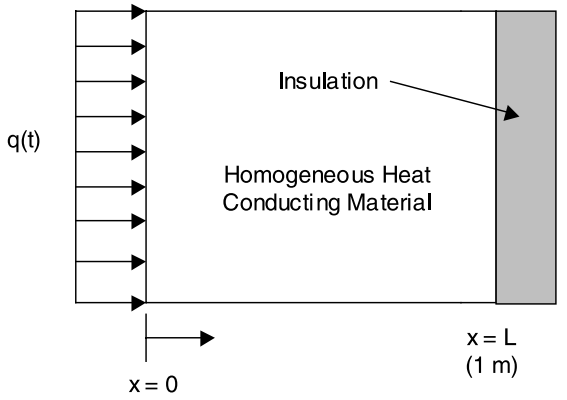

Fig. 1. One-dimensional heat conduction problem.

$$T(x,0) = T_0, \qquad 0 \leqslant x \leqslant L, \quad t = 0. \tag{4}$$

In order to solve the equations using finite-difference approximations, the heat conducting material is broken up into finite control volumes. Using the above equations, energy balances are performed on each control volume to determine the appropriate temperature relationship at each node. The resulting finite-difference equations are written in matrix form as

$$\dot{\mathbf{T}} = \mathbf{K}\mathbf{T} + \mathbf{R}\mathbf{q}, \tag{5}$$

where for six nodes

$$\mathbf{K} = \left(\frac{\alpha}{\Delta x^2}\right)\begin{bmatrix} -2 & 2 & 0 & 0 & 0 & 0 \\ 1 & -2 & 1 & 0 & 0 & 0 \\ 0 & 1 & -2 & 1 & 0 & 0 \\ 0 & 0 & 1 & -2 & 1 & 0 \\ 0 & 0 & 0 & 1 & -2 & 1 \\ 0 & 0 & 0 & 0 & 2 & -2 \end{bmatrix},$$

$$\mathbf{T} = [\,T_1(t) \quad T_2(t) \quad T_3(t) \quad T_4(t) \quad T_5(t) \quad T_6(t)\,]^{\mathrm{T}},$$

$$\mathbf{R} = \left[\left(\frac{2}{\rho c_p \Delta x}\right) \quad 0 \quad 0 \quad 0 \quad 0 \quad 0\right]^{\mathrm{T}},$$

$$\mathbf{q} = [q(t)].$$

In a standard (direct) heat transfer problem, the $\mathbf{K}$, $\mathbf{R}$ and $\mathbf{q}$ terms are known and $\mathbf{T}$ is determined through integration. For the inverse problem, $\mathbf{K}$ is known with some or all of the temperatures, $\mathbf{T}$, but the forcing term $\mathbf{q}$ is unknown. To solve the inverse problem, the continuous state–space relationship, Eq. (5), is converted into a discrete-time model using an appropriate numerical algorithm

$$\mathbf{T}^{j+1} = \mathbf{M}(h)\mathbf{T}^j + \mathbf{P}(h)\mathbf{q}^j, \tag{6}$$

where h is the time-step. Eq. (6) defines both the direct and inverse heat conduction problems. By applying a unit heat pulse at the boundary, (6) can be used to generate Duhamel's integral in discrete form as

$$\begin{bmatrix} T_i^2 & 0 & 0 & 0 & \cdots & 0 \\ T_i^3 & T_i^2 & 0 & 0 & \cdots & 0 \\ T_i^4 & T_i^3 & T_i^2 & 0 & \cdots & 0 \\ T_i^5 & T_i^4 & T_i^3 & T_i^2 & \cdots & 0 \\ \vdots & \vdots & \vdots & \vdots & \ddots & 0 \\ T_i^N & T_i^{N-1} & T_i^{N-2} & T_i^{N-3} & \cdots & T_i^2 \end{bmatrix}\begin{bmatrix} q^1 \\ q^2 \\ q^3 \\ q^4 \\ \vdots \\ q^{N-2} \end{bmatrix} = \begin{bmatrix} \theta_i^2 \\ \theta_i^3 \\ \theta_i^4 \\ \theta_i^5 \\ \vdots \\ \theta_i^N \end{bmatrix}, \tag{7}$$

where T_i^j is the temperature at node i for time j due to the heat pulse applied at the boundary at time zero, q^j is the actual heat flux at the boundary at time j and θ_i^j is the actual temperature at node i for time j. T_i^0 and T_i^1 were omitted from (7) because from it takes two time-steps for the pulse to affect the temperature at the location of interest. Since q^j enters the equation for $\boldsymbol{\theta}_i^j$ through the term $\mathbf{T}_i^0 \cdot \mathbf{q}^j$, it follows that $T_i^0, T_i^1 = 0$.

Eq. (7) can be expressed in matrix form as

$$\boldsymbol{\Phi}\mathbf{q} = \boldsymbol{\theta}. \tag{8}$$

The inverse heat conduction problem (IHCP) can be cast as solving for $\mathbf{q}$ given $\boldsymbol{\Phi}$ and $\boldsymbol{\theta}$. Because $\boldsymbol{\Phi}$ is ill conditioned, the IHCP cannot be solved by direct inversion. A variety of methods have been proposed to solve the inverse problem. However, a widely accepted method for solving problems involving ill-conditioned matrices is to employ singular-value decomposition (SVD) to compute the pseudo-inverse of $\boldsymbol{\Phi}$ [21]. To the authors' knowledge, this technique, that is well understood, easily implemented and direct, has not been employed to solve IHCPs. The rest of this article focuses on the physical meaning of each step in the SVD-pseudo-inverse procedure to provide insights into the IHCP. First, a brief overview of SVD is provided.

The decomposition consists in expressing $\boldsymbol{\Phi}$ as a product of two orthonormal matrices $\mathbf{U}$ and $\mathbf{V}$, and a diagonal matrix $\mathbf{S}$ as follows:

$$\boldsymbol{\Phi} = \mathbf{U}\mathbf{S}\mathbf{V}^{\mathrm{T}}. \tag{9}$$

The diagonal elements of the diagonal matrix $\mathbf{S}$ are called "singular values" and are usually arranged inside $\mathbf{S}$ in descending order. The condition number of a matrix is defined by

$$\mathrm{CN} = \frac{\text{largest singular value}}{\text{smallest singular value}}. \tag{10}$$

Matrices with large values ($\gg 1$) of condition number are ill conditioned. The matrix $\boldsymbol{\Phi}$ can be "reconditioned" by eliminating rows and columns from $\mathbf{S}$ corresponding to small singular values. If $\mathbf{S}$ is reduced in size, the corresponding $\mathbf{U}$ and $\mathbf{V}$ matrices must be reduced by the same amount. For example, assume there are 36 temperature readings at a given location within the system

$$\begin{array}{ccccccc} \boldsymbol{\theta} & = & \mathbf{U} & \mathbf{S} & \mathbf{V}^{\mathrm{T}} & \mathbf{q} \\ 36\times 1 & & 36\times 36 & 36\times 36 & 36\times 36 & 36\times 1. \end{array} \tag{11}$$

The singular-value matrix is used to reduce the model size by comparing the singular values. Columns and rows of $\mathbf{S}$ containing relatively small singular values are removed until the condition number is appropriate. Since $\mathbf{S}$ multiplies $\mathbf{U}$ and $\mathbf{V}^{\mathrm{T}}$, the corresponding columns removed from $\mathbf{S}$ are removed from $\mathbf{U}$ and $\mathbf{V}$. Assuming all but four singular values were removed, Eq. (11) is written using the reduced-order matrices

$$\begin{array}{ccccccc} \boldsymbol{\theta} & = & \mathbf{U}_{\mathrm{new}} & \mathbf{S}_{\mathrm{new}} & \mathbf{V}_{\mathrm{new}}^{\mathrm{T}} & \mathbf{q} \\ 36\times 1 & & 36\times 4 & 4\times 4 & 4\times 36 & 36\times 1. \end{array} \tag{12}$$

By comparing Eqs. (11) and (12), the reduction in size of the matrices involved is clearly evident. The direct problem involves applying Eq. (11) to obtain the temperature profile ($\boldsymbol{\theta}$) for a given heat flux profile ($\mathbf{q}$). In the inverse heat conduction problem, $\boldsymbol{\theta}$ is specified and Eq. (12) is solved for $\mathbf{q}$

$$\mathbf{q} = \mathbf{V}_{\mathrm{new}}\mathbf{S}_{\mathrm{new}}^{-1}\mathbf{U}_{\mathrm{new}}^{\mathrm{T}}\boldsymbol{\theta}. \tag{13}$$

3. Interpretation of singular value decomposition applied to inverse heat conduction problems

Since the rows of $\mathbf{U}$ are orthonormal it follows that $\boldsymbol{\theta} = \mathbf{U}[\mathbf{U}^{\mathrm{T}}\boldsymbol{\theta}]$. If the columns of $\mathbf{U}$ were obtained by discretizing appropriate sine waves then $\mathbf{U}^{\mathrm{T}}\boldsymbol{\theta}$ will contain the frequency components from the Fourier series of $\boldsymbol{\theta}$. The data are filtered by selectively removing frequency components from $\mathbf{U}^{\mathrm{T}}\boldsymbol{\theta}$, e.g., employing $\mathbf{U}_{\mathbf{new}}^{\mathrm{T}}\boldsymbol{\theta}$. The filtered temperature data are recovered from the truncated data through the following equation from the original temperature data:

$$\boldsymbol{\theta}_{\mathrm{filtered}} = \mathbf{U}_{\mathrm{new}}\left[\mathbf{U}_{\mathrm{new}}^{\mathrm{T}}\boldsymbol{\theta}\right]. \tag{14}$$

To investigate what type of filtering is taking place in the SVD approach, the columns of $\mathbf{U}$ and their power spectrum are plotted, Figs. 2 and 3, respectively. The profiles presented in Fig. 2 indicate the columns of $\mathbf{U}$ are sinusoidal-like with increasing frequency with respect to column number. Fig. 3 illustrates that each row contains a very narrow band of frequencies. Therefore, each row of $\mathbf{U}$ acts upon the measured temperature, $\boldsymbol{\theta}$, as a band-pass filter. The frequencies corresponding to the maximum amplitude of each band-pass filter are plotted against the corresponding singular values in Fig. 4.

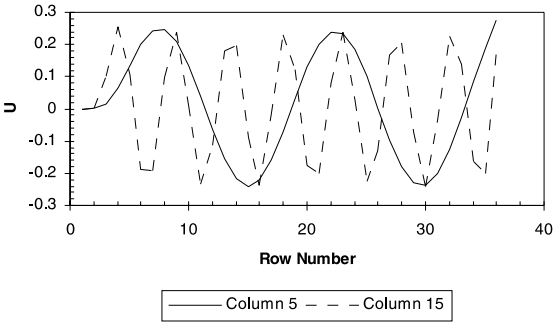

Fig. 2. Columnar values of $\mathbf{U}$.

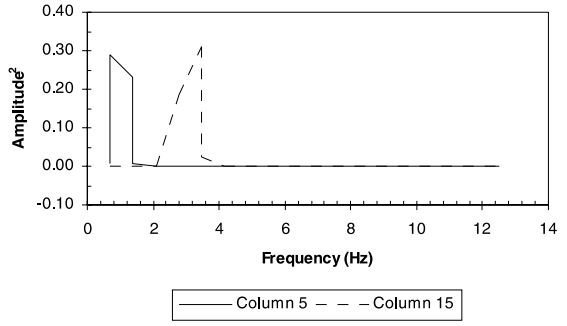

Fig. 3. Power spectrum of **U**.

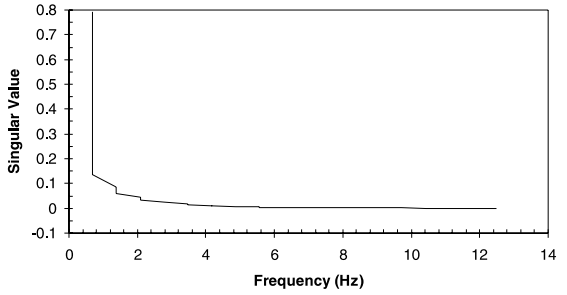

Fig. 4. Diagonal values of **S** (diagonals of **S** versus frequency, rows 1–35).

The second step involves determining the number of frequencies to be truncated. This is done by looking at the singular values and considering the signal-to-noise ratio contained in **θ**, Fig. 4. The last two singular values are zero within numerical precision and this is consistent with the delay time in the pulse affecting the location of interest. The inversion process in (14) requires obtaining the reciprocal of the singular values. Small singular values will result in large reciprocals that will amplify corresponding frequency components. Fig. 5 shows the degree of amplification versus frequency. Noise in the temperature data will also be amplified. The number of required columns and rows in $\mathbf{S}_{new}$ can be determined by considering the amplification factor of the reciprocal singular values and the signal-to-noise ratio.

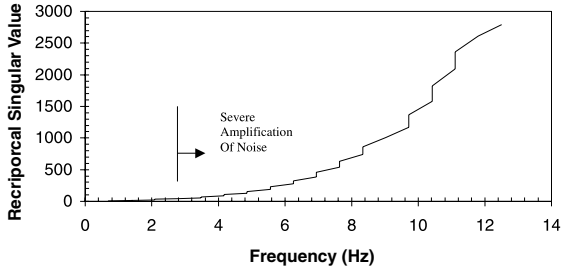

Fig. 5. Inverse of **S** diagonal (reciprocal of **S** versus frequency, rows 1–33).

4. Example application

To illustrate the matrix-transform method a standard test problem [13] is investigated. Consider the one-dimensional problem shown in Fig. 1. A known triangular heat flux as shown in Fig. 6 is applied to the left boundary and the temperature is recorded at the insulated boundary ($x = 1$ m).

For the purpose of this example the temperature data are computed for the triangular heat flux using the forward problem as expressed by Eq. (6), where **M** and **P** are determined using an exact exponential series employing a first-order-hold on heat flux, Fig. 7

$$\begin{aligned}\mathbf{M}(h) &= \mathrm{e}^{\mathbf{K}h} = \mathbf{I} + \mathbf{K}h + \frac{\mathbf{K}^2h^2}{2!} + \frac{\mathbf{K}^3h^3}{3!} + \cdots,\\ \mathbf{P}(h) &= \mathbf{K}^{-1}[\mathbf{M}(h) - \mathbf{I}]\mathbf{R}\\ &= \left[\mathbf{I}h + \frac{\mathbf{K}^2h^2}{2!} + \frac{\mathbf{K}h^3}{3!} + \cdots\right]\mathbf{R}.\end{aligned} \tag{15}$$

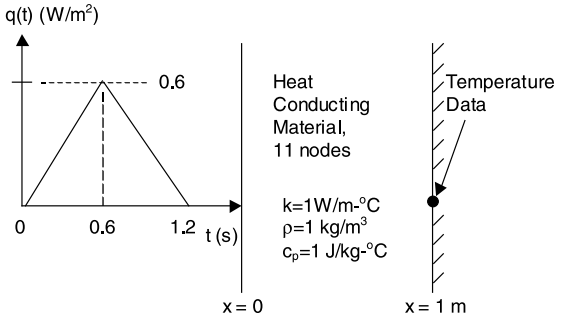

Fig. 6. Heat flux profile and recorded temperature location.

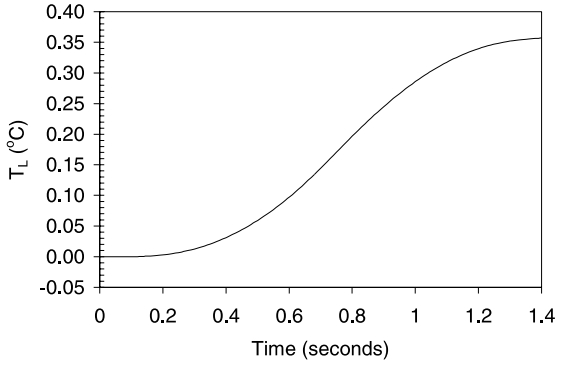

Fig. 7. Temperature history at insulated boundary (temperature at $x = L$ versus time, $\Delta x = 0.1$ m).

These temperature data are used in the inverse problem to try to recover the heat flux history, Fig. 8. Since the temperature will be extremely precise under these ideal conditions, the recovered heat flux profile should closely reproduce the triangular profile.

Fig. 8 illustrates the results for the recovered heat flux when $\Delta x = 0.1$ m. The results of using three different time-step sizes were compared. Without noise, truncation of singular values is mainly based on numerical precision; this translates to limiting the magnitude of the inverses of the singular values, Table 1. Removing as many as a hundred "high-frequency" singular values has negligible effect on the solution as shown for a time-step of 0.01 s.

The performance of the proposed method is demonstrated by adding a large component of noise (standard deviation equal to 10% of full scale) to the temperature data, Fig. 9. Only frequencies with good signal-to-noise ratios can be recovered with fidelity. This fact is used to determine the number of singular values to be used. To this end, the signal and noise power spectrums are compared in Fig. 10. In actual practice, the signal and noise spectrums can be estimated from the measured noisy data by standard signal processing techniques based on autocorrelation/covariance analysis [23]. Alternatively, a rough estimate of the noise strength can be obtained from steady-state measurements or from the higher-frequency components of the measured data. The latter statement reflects the fact that at higher frequencies the noise is expected to dominate the signal.

The recovered heat flux profiles are presented in Fig. 11. The error between the exact and calculated heat flux with 10% full-scale temperature noise is presented in Fig. 12. Table 2 summarizes the model-reduction process for these noisy data. Since only frequencies with good signal-to-noise ratios can be recovered, the reduced models for the noisy data are seen to be quite small. Frankel and Keyhani [8] demonstrated a similar reduction in model size.

In spite of the very noisy data and the seemingly several orders of the model reduction, Fig. 11 shows and compares the estimated versus the original heat fluxes. Some rounding of the corners is observed; however, this cannot be avoided because the noise obscures this detail. The solution is optimal in the least-squares sense since only orthogonal components of the physical model as-

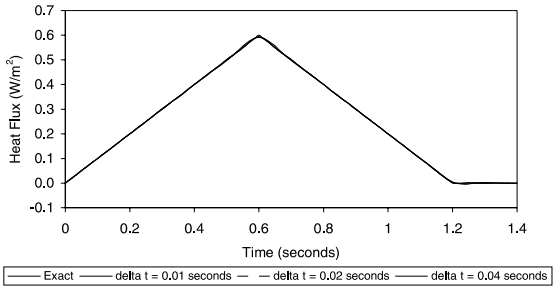

Fig. 8. Recovered heat flux profiles using exact temperature data (heat flux at $x = 0$ versus time, $\Delta x = 0.1$ m).

Table 1
Matrix dimensions using exact data as input

Time-step (s)	Number of time-steps	Size, $\mathbf{\Phi}$	Size, $\mathbf{S}_{new}$
0.01	144	(144×144)	(44×44)
0.02	72	(72×72)	(32×32)
0.04	36	(36×36)	(21×21)

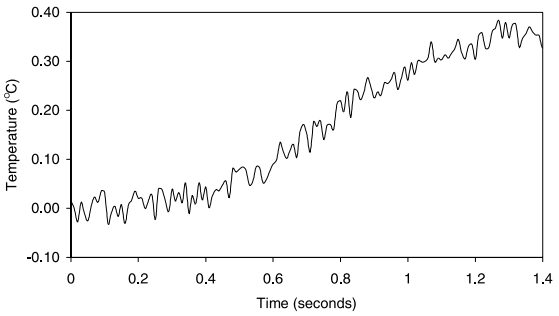

Fig. 9. Noisy temperature input (noisy temperature at $x = L$ versus time).

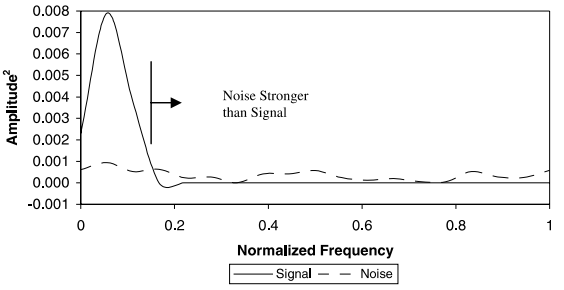

Fig. 10. Signal and noise power spectrum plot.

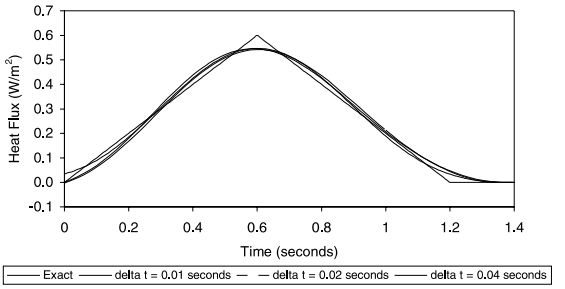

Fig. 11. Recovered heat flux profiles using noisy temperature data (heat flux at $x = 0$ versus time, $\Delta x = 0.1$ m).

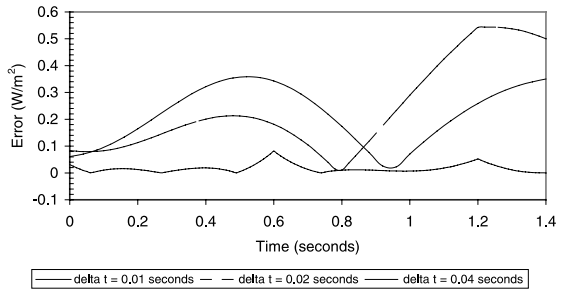

Fig. 12. Heat flux error versus time with input noise of 10% full-scale (heat flux error versus time, $\Delta x = 0.1$ m).

Table 2
Matrix dimensions using noisy data as input

Time-step (s)	Number of time-steps	Size, $\mathbf{\Phi}$	Size, $\mathbf{S}_{new}$
0.01	144	(144×144)	(4×4)
0.02	72	(72×72)	(4×4)
0.04	36	(36×36)	(4×4)

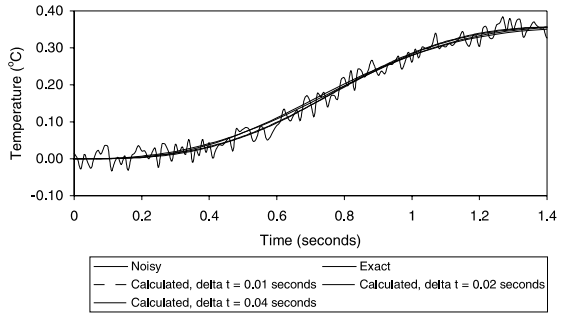

Fig. 13. Exact, noisy and calculated temperature profiles at $x = L$ (temperature at $x = L$ versus time, $\Delta x = 0.1$ m).

sociated with unreliable data are discarded. Fig. 13 shows a comparison of the noisy temperatures, the original temperatures and those calculated using the forward model and the recovered heat flux shown in Fig. 11.

5. Conclusions

The model reduction method provides an efficient numerical method for solving inverse heat conduction problems. Results using standard test problems indicate that heat flux estimates can be obtained using very noisy temperature data by properly conditioning the inverse problem using a reduced-order system of matrices. The matrix transform model provides two main advantages for solving inverse heat conduction problems. First, the reduced-order matrices allow heat flux estimates to be obtained from temperature data containing large amounts of noise. Second, there are no ad hoc parameters to specify for the filtering process to provide reasonable results.

References

[1] G. Stolz Jr., Numerical solutions to an inverse problem of heat conduction for simple shapes, J. Heat Transfer (1960) 20–26.
[2] J.V. Beck, B. Blackwell, C. St. Clair Jr., Inverse Heat Conduction: Ill-posed Problems, Wiley, New York, 1985.
[3] J.V. Beck, B. Blackwell, A. Haji-Sheikh, Comparison of some inverse heat conduction methods using experimental data, Int. J. Heat Mass Transfer 39 (7) (1996) 3649–3657.
[4] G. Blanc, J.V. Beck, M. Raynaud, Solution to the inverse heat conduction problem with a time-variable number of future measurements, Numer. Heat Transfer, Part B 32 (1997) 437–451.
[5] H. Reinhardt, Analysis of sequential methods of solving the inverse heat conduction problem, Numer. Heat Transfer, Part B 24 (1993) 455–474.
[6] G.P. Flach, M.N. Ozisik, An adaptive inverse heat conduction method with automatic control, J. Heat Transfer 114 (1992) 5–13.
[7] E.P. Scott, J.V. Beck, Analysis of the sequential regularization solutions of inverse heat conduction problems, J. Heat Transfer 111 (1989) 218–224.
[8] J.I. Frankel, M. Keyhani, A global time treatment for inverse heat conduction problems, J. Heat Transfer 119 (1997) 673–683.
[9] J. Blum, W. Marquardt, An optimal solution to inverse heat conduction problems based on frequency-domain interpretation and observers, Numer. Heat Transfer, Part B 32 (1997) 453–478.
[10] W. Marquardt, H. Auracher, An observer-based solution of inverse heat conduction problems, Int. J. Heat Mass Transfer 33 (7) (1990) 1545–1562.
[11] E. Bayo, H. Moulin, O. Crisalle, G. Gimenez, Well-conditioned numerical approach for the solution of the inverse heat conduction problem, Numer. Heat Transfer, Part B 21 (1992) 79–98.
[12] H.C. Moulin, E. Bayo, Well-conditioned numerical method for the nonlinear inverse heat conduction problem, Numer. Heat Transfer, Part B 22 (1992) 321–347.
[13] D.M. Trujillo, H.R. Busby, Practical Inverse Analysis in Engineering, CRC Press, New York, 1997.
[14] A.N. Tikhonov, V.Y. Arsenin, Solution of Ill-posed Problems, Winston, Washington, DC, 1977.
[15] R.E. Kalman, A new approach to linear filtering and prediction problems, ASME J. Basic Eng., Ser. 82d (1960) 35–45.
[16] P. Tuan, C. Ji, L. Fong, W. Huang, An input estimation approach to on-line two-dimensional inverse heat conduction problems, Numer. Heat Transfer, Part B 29 (1996) 345–363.
[17] C. Ji, H. Jang, Experimental investigation in inverse heat conduction problem, Numer. Heat Transfer, Part A 34 (1998) 75–91.

[18] M.N. Ozisik, H.R.B. Orlande, Inverse Heat Transfer Fundamentals and Applications, Taylor & Fracis, New York, 2000.
[19] M.J. Colaco, H.R.B. Orlande, Comparison of different versions of the conjugate gradient method of function specification, Numer. Heat Transfer, Part A 36 (1999) 229–249.
[20] C. Huang, S. Wang, A three-dimensional inverse heat conduction problem in estimating surface heat flux by conjugate gradient method, Int. J. Heat Mass Transfer 42 (1999) 3387–3403.
[21] R.L. Burden, J.D. Faires, Numerical Analysis, PWS-Kent, Boston, MA, 1981.
[22] G. Strang, Linear Algebra and its Applications, Saunders, New York, 1988.
[23] L.R. Rabiner, B. Gold, Theory and Application of Digital Signal Processing, Prentice-Hall, Englewood Cliffs, NJ, 1975.